Response to the Review on the Paper wes-2021-30-RC1

Investigation Into Boundary Layer Transition Using Wall-Resolved LES and Modeled Inflow Turbulence

B.A. Lobo, A.P. Schaffarczyk, M. Breuer

Review # 1

We appreciate the effort of the reviewer for evaluating our manuscript in detail. In the following his/her remarks are answered and modifications resulting from his/her comments are explained. Note that in the annotated version of the manuscript all modifications (replacements, additions and deletions) regarding the remarks of reviewer # 1 will be highlighted in red when the upload of an annotated version is an option.

Response to specific comments:

- **Simulation matches the test section of the experimental study by Reichstein et al. (2019) but no comparisons have been made**
  The reviewer is right and the airfoil used for the present simulations corresponds to the test section of the experiment by Reichstein et al. (2019). However, no direct comparison of the current results with this experiment have been made since the present simulation is carried out at a Reynolds number of 100,000, whereas the experiment is conducted at a Reynolds number in the order of a few millions.

  Further information: Future simulations at higher Reynolds numbers and in comparison to that of the experiment are being carried out. The reason for running a first simulation at a relatively low Reynolds number of 100k and then stepping up the Reynolds number incrementally is because transitional studies using wall-resolved LES around airfoils for Re numbers in the order of a few millions are rarely available.

- **Comparison with XFOIL**
  The reviewer is right. A comparison with XFOIL would be helpful for serving as a benchmark to the readers. Fig. 1 (at the end of this document) shows the pressure coefficient plot with the results predicted by XFOIL included. This will be added to the next version of the manuscript.

  Note: In the current version of the manuscript there was an error in the plotting of the pressure coefficient. The reference pressure was not taken into consideration and this will be changed in the second version before publication. This does not affect any of the results or calculations other than the plot of the lift-to-drag ratio, which will also be updated. The corrected lift-to-drag plot can be seen in Fig. 2.

- **Comparison with the work of Breuer (2018) and Breuer and Schmidt (2019)**
  More information comparing the results with the previous study is a good suggestion and more information will be added to the next version of the manuscript. The following points will be added where appropriate. A short summary is as follows:

  On the relatively thinner airfoil (8.51 %) in the study by Breuer (2018), separation takes place close to the leading edge at around 20 % chord and moves downstream

with increasing turbulence intensity. Furthermore, a corresponding reduction in the chordwise extension of the separation bubble is seen before it disappears at a TI of 5.6 %. The time-averaged results showed a decrease in the drag coefficient with increasing TI. A more detailed analysis revealed that the contribution of the pressure component decreased due to the reduction in the length of the separation bubble while that of the friction component increased due to increasing inflow TI. In the current study on the flow around the thicker (20 % thickness) LM45 airfoil, the separation bubble moves slightly downstream with increasing TI before disappearing at a TI of 11.2 %. However, here the length of the separation bubble does not decrease with increasing TI. The absence of a separation bubble at a TI of 11.2 % is due to the increased momentum exchange within the boundary layer with the flow being transitional and closer to the turbulent regime than the laminar regime at the location, where it would have otherwise separated. Correspondingly, a resulting increase of the drag coefficient with increasing TI is seen.

In the study by Breuer (2018) a decrease in the lift coefficient is observed with an increase in TI up to 5.6 % before it stays constant. It is known that a separation bubble close to the leading edge could increase the lift coefficient due to the increase in the apparent camber caused by the presence of the separation bubble. With increasing TI and the downstream shift of the separation bubble, the lift coefficient then decreases. In the present study, the lift coefficient increases with increasing TI, however very slightly (a relative change of 3 %) and is likely caused by the slight downstream shift of the separation region, which increases the extent of the laminar flow along the chord.

A combination of these factors results in an increasing lift-to-drag ratio with increasing TI in Breuer (2018), whereas the lift-to-drag ratio in the current study reduces.

- **Grid resolution - Comparison of the actual values computed**
  Figure 3 of this reply shows a comparison of the pressure coefficient between the standard and the refined grid with about three times more grid points. With the refined grid the separation bubble can easily be identified by the flattened c_p curve. The corresponding c_f plot can be seen in Fig. 4 of this reply. Again, some deviations between the results on both grids are visible. However, for the current study which is focused on the transition phenomena, the standard grid provides a sufficiently accurate resolution with no significant changes observed in the mode of transition as seen in Fig. 1 of the manuscript. Please additionally note that the suction side is of special interest in our study and it has a finer grid resolution than the pressure side. Details are found in Table 2 of the manuscript. Taking into account the goal of the present study and the very high computational costs already necessary for the long-lasting time-consuming predictions on the standard grid, the present resolution is deemed to be sufficient for the purpose of this study.

- **High-frequency component in Fig. 1 around the mid-blade**
  The high frequency components around the mid-blade are caused by numerical noise. They are only visible near the region of breakdown to turbulence and according to our analysis do not directly affect the transition process. The cause cannot be easily isolated since in the case of an unstable system even the smallest disturbances caused by round-off errors could be a possible reason. The present simulations are carried out

with REAL*8 accuracy yielding an accuracy up to 12 or 13 digits, so this reason is unlikely. Other larger sources of disturbances are convergence errors. In the present code the Poisson equation for the pressure correction is solved based on an iterative method, i.e., the incomplete LU decomposition method of Stone (1968). The iteration is stopped if the mass conservation is fulfilled up to a convergence criterion of about 10^{-9}. Thus, it is not exact and induces disturbances. A third possible source of disturbances is due to modeling errors by the dynamic subgrid-scale model. Finally, also some minor numerical oscillations due to the application of the central second-order accurate scheme can not be fully excluded. That scheme has the advantage of low numerical dissipation, which is important for LES. On the other hand, it is prone to numerical oscillations. Unfortunately, all these errors can not be clearly separated. Hence, it is impossible to give the real reason.

- **Addition of a grid to some figures**
  A grid or axis will be included in those images, where it is presently absent in order to improve the readability.

- **Input from Reichstein (2019) experiments for the length and time scales**
  The length and time-scales were chosen from the experiment by Hain et al. (2009) due to the similar order of magnitude of the Reynolds number. The second and more important reason for this choice is the fact that the scales from the experimental data are very large and would require a large computational domain also in the spanwise direction (up to 8 times the chosen spanwise extension) which would make the task computationally infeasible.

  Further information: For future simulations at higher Reynolds numbers as discussed above, the anisotropic inflow turbulence will be generated based on the Kaimal formulation (IEC61400-1) wherein the length/time scales are relatively determined based on a single integral scale. In this case, the scales will be determined based on the spanwise extent of the domain and not on the experimental data, again due to the computational costs being a limiting factor.

- **Clarification on what dimensionless units refer to**
  All the dimensions are non-dimensionalized with respect to the inflow velocity u_∞ and the chord length c as mentioned in the manuscript.

- **Figure 2 comparison to the Kolmogorov -5/3 spectrum**
  The next version of the manuscript will be updated with a plot showing the Kolmogorov -5/3 slope. This can be already seen in Fig. 5 of this reply.

- **Definition of the shape factor**
  The definition of the shape factor can be found on line 300 of the original manuscript. It is defined as the ratio between the displacement thickness and the momentum thickness.

- **Good correlation in the transition location (line 313)**
  Thanks to the reviewer for pointing this out. Line 307 needs to be explained a bit better. A corresponding change will be made to the second version of the manuscript. What is meant on line 307 is that the crucial transition onset is seen not at the point of

minimum friction coefficient c_f, but somewhere in-between the region where it begins to drop (around 58 % chord at a TI of 0 %) and the point of minimum c_f (around 64 % chord at a TI of 0 %). This is in good correlation with the maximum of the shape factor. It must further be pointed out that these are just common methods used in the literature and it is difficult to pick a specific point as the location for the onset of transition. Therefore, the two methods are not expected to provide exactly the same chordwise position. However, we do see a very good correlation with transition being in a similar region and the change in the transition location with varying inflow turbulence also being reflected by both the c_f plot and the plot of the shape factor.

- **Figure 5 uf to u′**
  Yes, that is correct. uf = u'. The legend will be changed to reflect this in the next version.

- **Diwan and Ramesh flat plate**
  The reviewer is right. The experimental and theoretical study by Diwan and Ramesh (2009) was conducted on a flat plate. However, it was set-up in a wind tunnel such that there was an imposed pressure gradient typical for an airfoil with separation. Due to the imposed pressure gradient the effects of curvature from a typical airfoil are seen on the flat plate. What we have learned from this experiment and our simulations is that in the region of an adverse pressure gradient (which is often caused by blade curvature) and at relatively low Reynolds numbers that allow for laminar flow separation, the region upstream of separation can already show the presence of inflectional instabilities. These instabilities are typically associated with the separated flow region due to an adverse pressure gradient but the study by Diwan and Ramesh and the present LES simulation shows that they can also be present in the attached flow, specifically, the region directly upstream of separation.

- **Figure 9f explanation**
  A short explanation of this image will be added to the manuscript around line 404 to 406. The text would change to: *"In order to follow the transition process even in the laminar separation region, data evaluations were carried out at the height of the boundary layer displacement thickness and at the mid-span. These locations have been marked and can be visualized in Fig. 9 f."*

- **Isotropic instead of atmospheric turbulence**
  Yes, the reviewer is right and the goal of the PhD project to which this simulation belongs is to ultimately study the effects of atmospheric turbulence at a high Reynolds number of about 1 million. However, as described above, the Reynolds number will be stepped-up incrementally. The second case is being run at a Reynolds number of 500k and the third case at a Re = 1M. In these cases anisotropic turbulence based on the Kaimal formulation (IEC61400-1) resembling atmospheric inflow will be used. In the present study isotropic turbulence was used to match previous studies at this Reynolds number (Hain et al. 2009, Breuer 2018, and Breuer and Schmidt 2019).

We gratefully acknowledge the effort of the referee and his/her contributions in enhancing

the quality of our paper. Thanks a lot.

B.A. Lobo, A.P. Schaffarczyk, M. Breuer

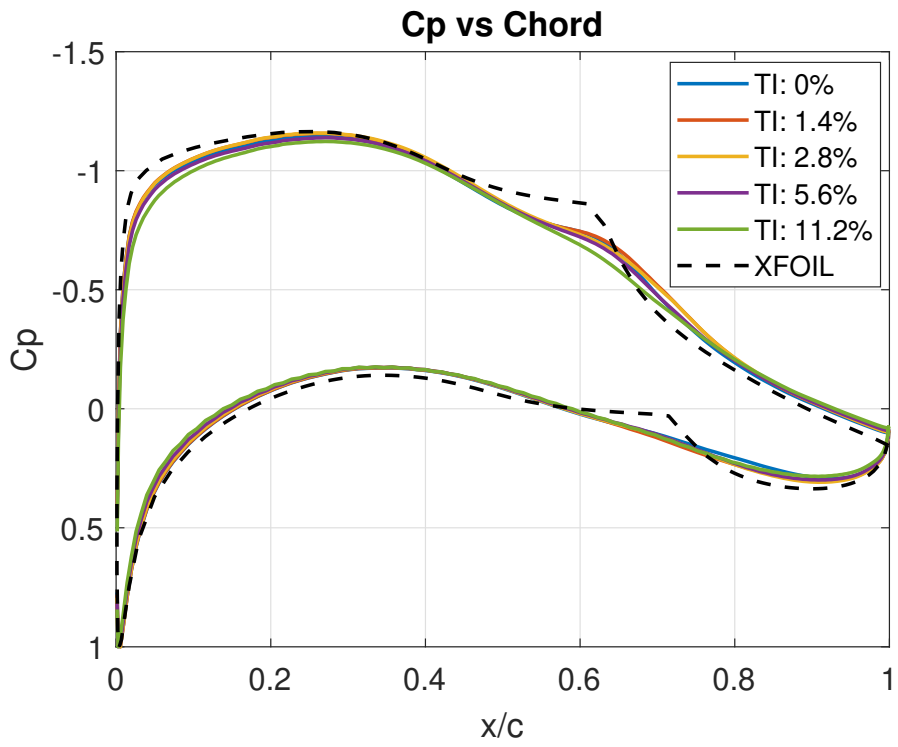

Figure 1: Pressure coefficient based on the averaged flow at different inflow turbulence intensities at a Reynolds number of 10^5 and $\alpha = 4°$.

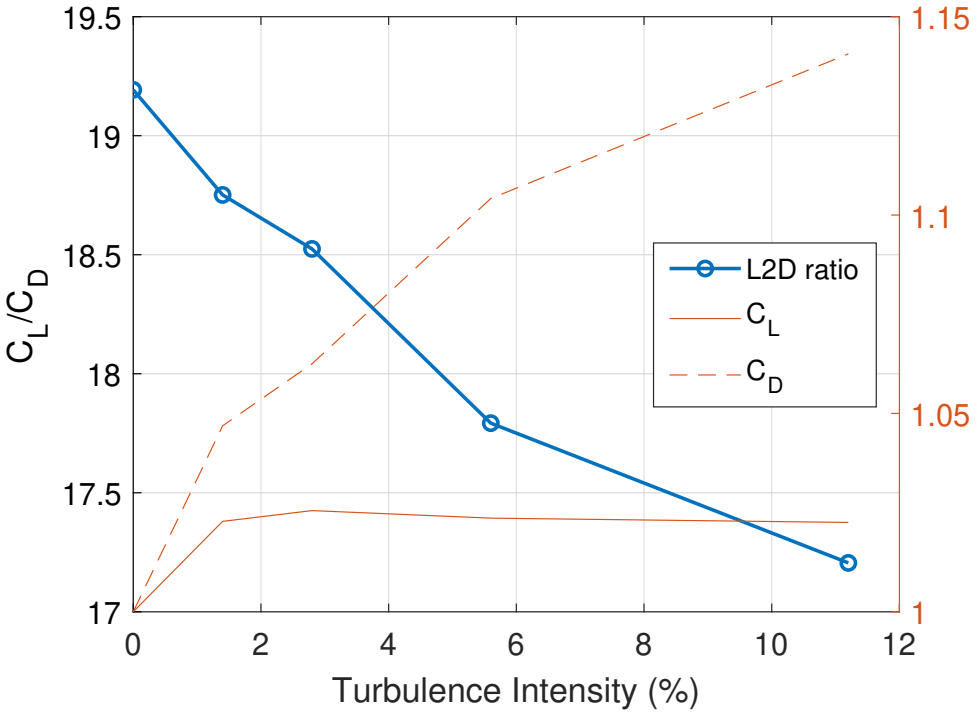

Figure 2: Distribution of the lift-to-drag ratio at different inflow turbulence intensities at a Re $= 10^5$ and $\alpha = 4°$. The right vertical axis shows the lift and drag coefficient scaled by the corresponding lift and drag coefficients of the reference case with a TI of 0 %.

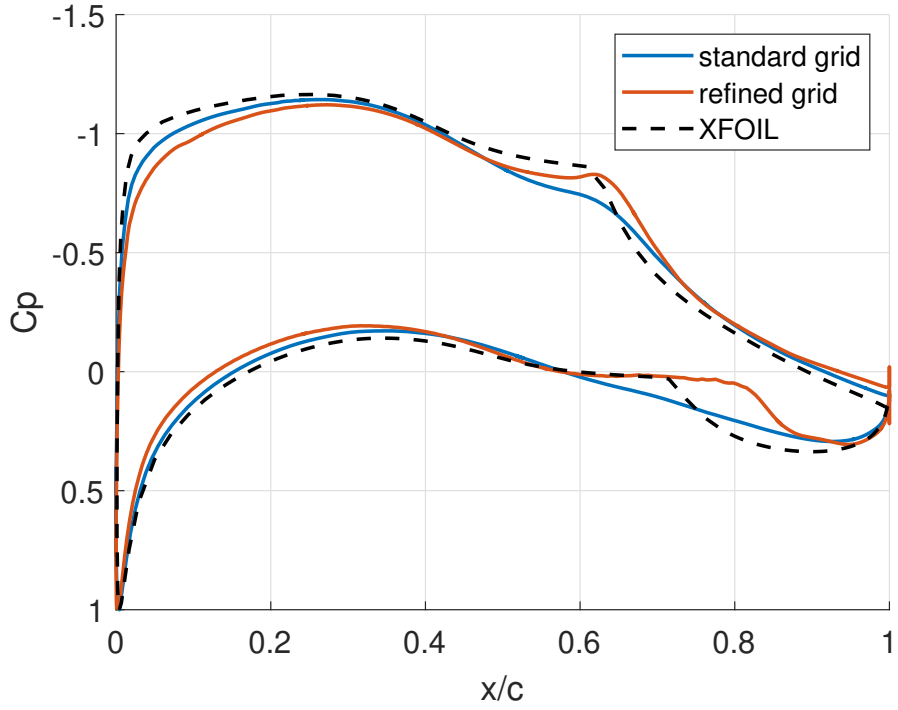

Figure 3: Pressure coefficient of the standard vs. the refined grid at a TI = 0 %.

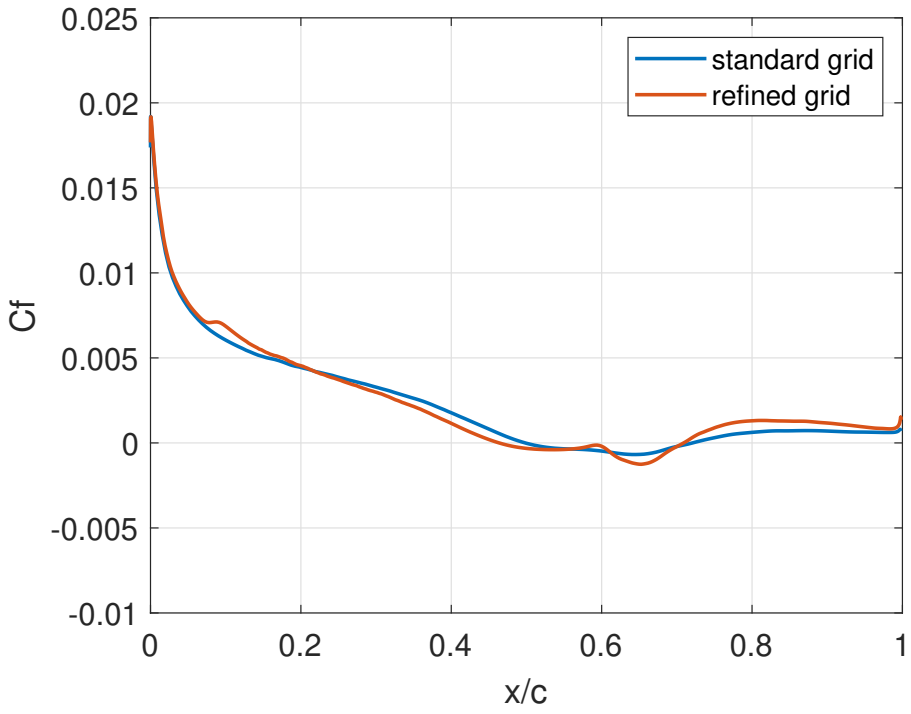

Figure 4: Friction coefficient of the standard vs. the refined grid at a TI = 0 %.

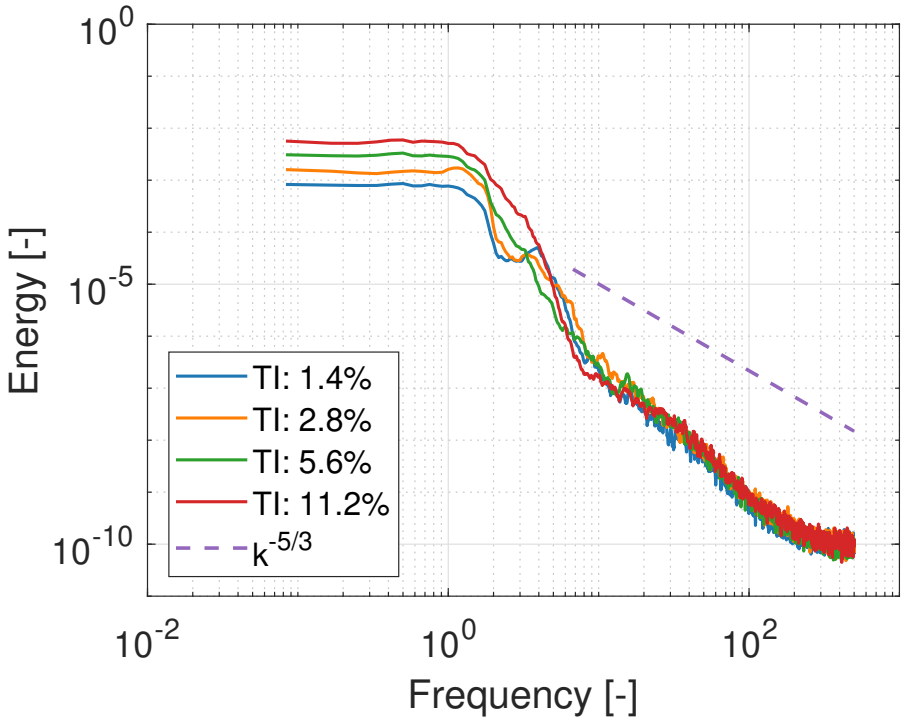

Figure 5: Turbulent kinetic energy spectra of the generated inflow turbulence.